# BACK-SUBSTITUTION BASED SPACECRAFT DYNAMICS MODELING WITH SELECTIVE CONFIGURATION SPACE BRANCHING

## Andrew Morell[*] and Hanspeter Schaub[†]

Traditional spacecraft designs include a collection of spacecraft components rigidly mounted to a common central hub. As new missions propose more complex architectures, performance gains are sought through mounting actuators to moving platforms instead of this central hub, achieving controllable degrees of freedom or longer moment arms. This added vehicle complexity must be met with modelling and simulation to support the increased dynamical complexity where the rigid assumption between a component and its central hub is removed. Spacecraft simulations which assume a traditional design about a central hub require adaptations to support the dynamical modelling of components branched off of other components. The Basilisk Simulation Framework is chosen as an existing modular framework specifically designed for spacecraft which leverages the back-substitution method (BSM). Mathematical alterations are made to Basilisk's back-substitution implementation of its "spinning bodies" moving platform model to allow the attachment of Basilisk's "dynamic effector" implementations of other components. This selective configuration space of branching enables components which exclusively generate forces and torques without a time varying geometry to be attached to such a time varying geometry. This attachment includes a two-way dynamical coupling where the moving platform updates the spatial states of components attached to it, and those attached components contribute their generated forces and torques directly to the moving platform. The dynamical differences between this branched architecture and a strictly hub centric implementation of the same parameters are highlighted through comparison of their resulting motion with a thruster attached. The branched design results in more intuitive motion of the motion platform flexing ahead of its central hub, whereas the traditional design results in the motion platform lagging behind its central hub.

## INTRODUCTION

Spacecraft structural architectures can be thought of as a set of components mounted to a central hub structure. Typically, components are mounted directly to this central hub and when the dynamics of the vehicle are modelled the assumption is made that this attachment is rigid. However, as modern space missions eye more ambitious goals, the complexity

[*]Graduate Research Assistant, Ann and H.J. Smead Department of Aerospace Engineering Science, University of Colorado, Boulder, 431 UCB, Colorado Center for Astrodynamics Research, Boulder, CO, 80309.

[†]Professor and Department Chair, Schaden Leadership Chair, Ann and H.J. Smead Department of Aerospace Engineering Sciences, University of Colorado, Boulder, 431 UCB, Colorado Center for Astrodynamics Research, Boulder, CO, 80309.

of their structural designs are also growing. Spacecraft components previously mounted statically to a central hub can be seen in mission concepts attached to mobile structures, and components with legacy being on mobile platforms can be seen on thinner or higher degree of freedom structures. These cases in which a component's attachment to its central hub is not considered rigid are referred to as time varying geometries and in the context of space missions can be grouped into some common categories of multi-body dynamics modelling considerations. This work considers three such categories corresponding to what modelled forces and torques drive the time varying geometries: actuated joints, hub excited flexing, and component excited flexing. Previous developments in the first two categories are highlighted, and the third category is proposed as a previously unexplored problem. The goal of all three categories is to improve the accuracy in modelling and simulation of how the spacecraft and its associated structures move.

In the case of actuated joints, components are mounted to an intermediate platform on the central hub in order to provide controllable degrees of freedom to the component. Forces and torques are directly applied at a joint to change what configuration a component is in, and reactionary forces and torques must be applied to the central hub. For example, solar arrays and communications antennas can be gimbaled in one or two degrees of freedom to enable more optimal vehicle pointing configurations. Thrusters are gimbaled on larger spacecraft to align thrust forces with the vehicle's center of mass minimizing undesired torque generation. Robotic arms can be thought of as a series of intermediate platforms, often with grappling end effectors used on vehicles performing docking operations. The dynamics of generalized multibody systems in the context of free flying spacecraft is thoroughly studied in the literature.[1–3] These structures are commonly assumed to be rigid bodies attached to the central hub with no flexing motion outside of what is allowed and commanded at the joint. When these rigid on rigid and purely controlled assumptions are made, their motion is considered to be prescribed meaning that a modelled intermediate platform moves along a planned path without considering external forces.[4,5]

While actuated joints assume rigid bodies connected by a rigid joint, the case of passively flexible structures is concerned with removing the rigid joint assumption to consider a rigid platform flexibility attached to a rigid central hub. In the case of hub excited flexing, the motion of a component platform lags behind the motion of its central hub due to natural stiffness and damping in the structure. In this work, the flexing is assumed to be first-order occurring only at the joint, with no deflection of the structures on either side of the joint preserving their rigid body assumption. Prior work has utilized some of the same methods used for modelling traditional multibody dynamics such as Kane's method[3] but with the joint loosened to a flexible assumption.[6,7] Therefore, the forces and torques of interest at the joint result from an excitation by the movement of the central hub. For example, non-actuated solar panels which are large with respect to their central hub may still move during a slew maneuver with respect to their central hub due to the underlying structure flexing. Other large yet thin passive components whose structural flexing is motivated to be dynamically modelled includes booms for gravity gradient stability and antennas.

The case of component excited flexing is applied to the same types of flexibly susceptible

structures outlined for hub excited flexing, but instead focuses on forces and torques applied by components of the flexible structure on the external environment. The flexing is still considered first-order occurring only at the attachment joint, but the central hub can be thought of as lagging behind in motion as the attached platform moves subject to its own external forces and torques. For example, a thruster mounted on the end of a robotic arm applies a directional force which first accelerates the arm before its forces and torques are passed through the arm's joints to the central hub. Consideration of this component excited flexing for a full spacecraft dynamical model is not found in prior literature.

This third category of component excited flexing is motivated by several new missions which are seeking better performance by mounting actuators on moving platforms rather than fixing them to the central hub. Two examples are Astroscale's Life Extension In-orbit (LEXI) spacecraft and Northrop Grumman's Mission Robotic Vehicle (MRV) and Mission Extension Pod (MEP) shown in Figure 1.[8,9] The LEXI spacecraft hosts four two-degree-of-freedom (2-DOF) arms with thrusters attached at the ends, and four other 2-DOF robotic arms for docking. The MEP is itself held by the MRV using two multi-DOF robotic arms, and then has its own singular multi-DOF robotic arm with a thruster mounted at the end. Other missions sporting similar use of robotic arms for docking include the European Space Agency's Clearspace-1, NASA's OSAM-1, and Starfish Space's Otter.[10–12] Each of these arms when fully extended have the potential to experience significant deflection when either thrust or grappling occurs at their ends.
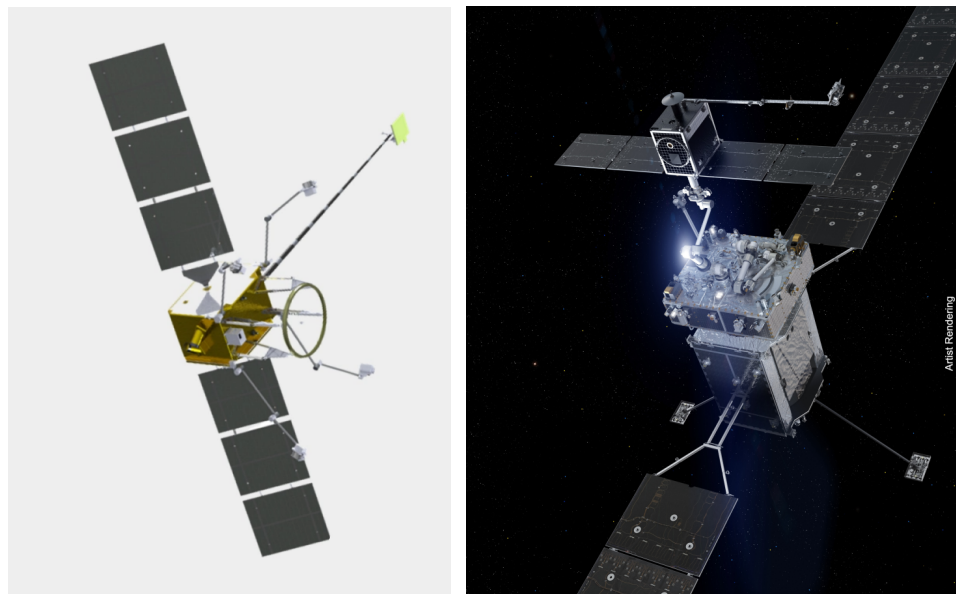


(a) Astroscale's LEXI [13].  (b) Northrop Grumman's MRV and MEP [14].

**Figure 1. Model renders of spacecraft component branching architectures.**

It is important to note that all three of the discussed categories of modelling forces and torques for actuated and passively flexing components are not mutually exclusive. Flexing of a structure about some nominally actuated configuration can be considered, achieving

a combination of the two modelling considerations. For example, a solar panel may be actuated to be pointing at different angles with respect to its central hub when that central hub performs orbital maneuvers, and therefore the resulting flexing would occur in different directions with respect to the hub-panel connection. Alternatively, if the central hub is inactive, not producing any external forces or torques on the environment, and instead quickly slews its solar panels to a different configuration, those panels could flex as their motion lags behind what is being commanded at the connection joint. This has historically been studied in the context of deployment maneuvers.[15,16]

How the dynamics of a space vehicle are modelled is largely dependent on the solver used and therefore the simulation framework in which they are implemented. When considering time varying geometries for a multi-body dynamical system, the equations of motion are a coupled nonlinear set which may be organized in different forms depending on the solving technique to be used. While a multitude of software packages leveraging different techniques exist, this project seeks simulation framework that is 1) computationally efficient at solving the coupled nonlinear equations, 2) tailored to spacecraft components and environments, and 3) open source such that the underlying dynamics solver is available to be adapted. Based on these criteria, the Basilisk Simulation Framework[*] is chosen which leverages the back-substitution method (BSM) to modularize a spacecraft's equations of motion.[17] Basilisk has already been applied to the component categories of actuated and hub excited time varying geometries.[5,16] While Basilisk's BSM is well tailored to the modular nature of spacecraft, it follows the common assumption first mentioned that spacecraft are organized as a set of components mounted to a central hub.[18] Therefore, the underlying technology required to model component excited flexing in a modular way is the ability to branch components.

The paper is structured as follows: The problem formulation outlines the exact challenges and their successive solutions followed by a mathematical overview of the required modifications to the BSM. Next, in the numerical results section, results showing platform deflection and corresponding hub motion for different thruster and arm configurations are be shown. Discussion as to the advantages of using each modelling category over another are provided, highlighting trades between complexity of model setup, computation time, and perceived accuracy.

**PROBLEM FORMULATION**

The goal to model component excited flexing is rooted in a more general problem: branching of components on a spacecraft. The goal is to not only model a specific instance of forces and torques applied to an intermediate moving platform, but to enable the connection of any component to a such moving platform which is a task in dynamical modelling at a more generalized scale.

The application of forces and torques along flexible structures proposes challenges in dynamical modelling, as some external forces and torques generated on a flexing structure

---

[*]`http://hanspeterschaub.info/basilisk`

must exert those external influences according to inertial states which are propagated at the central hub level. For example, forces and torques due to solar radiation pressure (SRP) on a large solar array or sail are dependent on the array's orientation with respect to the sun, so those computations become dependent on both the central hub's orientation and the panel's deflection at its joint to the hub. The challenge ultimately lies with ensuring that this dynamical linking preserves the modularity of Basilisk and provides a generalized solution.

The modularity of dynamics in Basilisk is achieved through utilizing the BSM. In order to expand the BSM to enable this component excited flexing, the modular architecture of Basilisk is adapted to allow components to be attached to moving platforms on a spacecraft rather than exclusively on a central hub. This branching off of components on other components is only applicable to selective configurations in Basilisk. In Basilisk, components are referred to as effectors and exist as two different types. There are dynamic effectors which only generate forces and torques such as a thruster, solar radiation pressure, drag, or the constraint effector used to model docking forces and torques. Then there are state effectors which in addition to generating forces and torques also have states to be integrated in the spacecraft's system of equations of motion such as the angle orientation of a moving platform or the speed of a reaction wheel. The expansion of the Basilisk Simulation Framework in this work enables dynamic effectors to be attached to a state effector, but does not enable a state effector to branch off of any other type of effector.
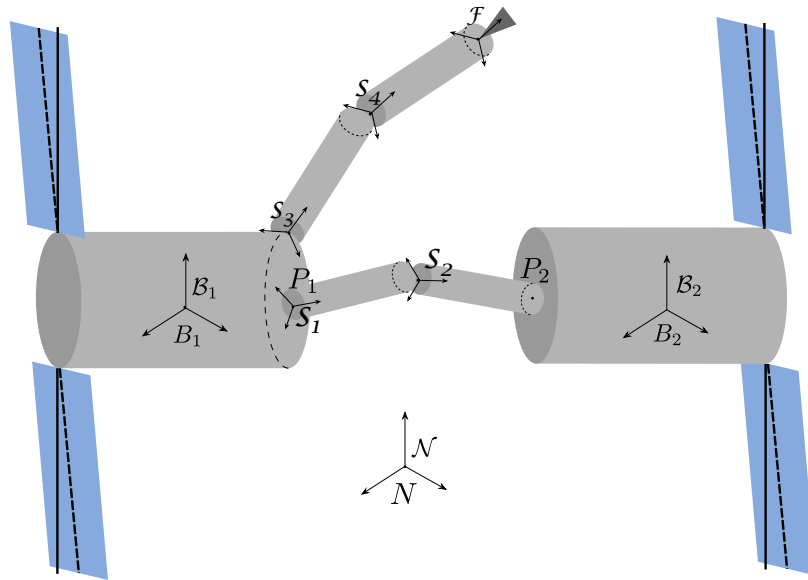


**Figure 2. Component branching example configuration.**

One example configuration is shown in Figure 2. There are two 2-DOF robotic arms: one connecting the two rigid hubs $B_1$ and $B_2$, and another mounting a thruster $\mathcal{F}$ to hub $B_1$. While not previously capable of being modelled by Basilisk, with component branching enabled it can be modelled in multiple ways. One way would be to consider $B_1$ as the central hub with two 1-DOF arms as its solar panels, one 2-DOF arm for the mounted

thruster, and one 5-DOF arm for $B_2$ and its panels. Another way would be to consider $B_2$ as the central hub, again with 2 1-DOF panels, but then with a 7-DOF arm modelling the connection to $B_1$ and its branched panels and thruster.

When arranging the dynamics of these different types of effectors into the BSM, Basilisk first sums the forces and torques of all dynamic effectors assuming them to act on the central hub. Then Basilisk compiles the contributions to the hub's translational and rotational states by state effectors. For component excited flexing, any dynamic effectors attached to a state effector must have their generated forces and torques summated and applied to the state effector's equations of motion before the residual is then passed through when said state effector has its contributions compiled by the central hub.

There are three collections of state effectors in Basilisk which are able to model a moving platform: hinged rigid bodies, linear translation bodies, and spinning bodies. Linear translation bodies models linearly translating platforms. The hinged rigid bodies are a collection of successive platforms connected by hinges that all lie in the same direction, whereas the spinning bodies are a collection of successive platforms connected by hinges that can be oriented in any direction. Spinning bodies is chosen to be adapted in this work given its ability to model any set of spinning bodies, including those that hinged rigid bodies is capable of. This behavior best matches robotic arms currently used in space, which rarely have linearly translating joints.

## MATHEMATICAL OVERVIEW OF BSM

To understand applying component excited flexing in the context of the BSM, it is beneficial to first lay out the relevant terms used in this method from Reference (18). Note that bold variables $x$ implies a vector quantity, $\dot{x}$ denotes an inertial frame relative time derivative of $x$, whereas $x'$ denotes a body frame relative time derivative, and $[\tilde{x}]y$ is the matrix cross product notation. Eq. (1) shows the compact form of the coupled translational and rotational EOMs of the spacecraft hub.

$$\begin{bmatrix} [A][B] \\ [C][D] \end{bmatrix} \begin{bmatrix} \ddot{\boldsymbol{r}}_{B/N} \\ \dot{\boldsymbol{\omega}}_{B/N} \end{bmatrix} = \begin{bmatrix} \boldsymbol{v}_{\text{Trans}} \\ \boldsymbol{v}_{\text{Rot}} \end{bmatrix} \tag{1}$$

Here $\ddot{\boldsymbol{r}}_{B/N}$ is the inertial translational acceleration between body fixed point $B$ on the spacecraft hub and inertially fixed point $N$, and $\dot{\boldsymbol{\omega}}_{B/N}$ is the inertial angular acceleration between body fixed frame $\mathcal{B}$ and inertially fixed frame $\mathcal{N}$. These translational and rotational EOMs of the spacecraft's central hub are decoupled from the states of other component effectors which are grouped into the matrices $[A]$, $[B]$, $[C]$, and $[D]$ and vectors $\boldsymbol{v}_{\text{Trans}}$ and $\boldsymbol{v}_{\text{Rot}}$ shown

in Eqs. (2a)-(3b).

$$[A] = m_{\text{sc}}\,[I_{3\times3}] + \sum_{i=1}^{N_{\text{eff}}} \boldsymbol{v}_{\text{Trans,LHS}_i}\,\boldsymbol{a}_{\alpha_i}^T \tag{2a}$$

$$[B] = -m_{\text{sc}}\,[\tilde{\boldsymbol{c}}] + \sum_{i=1}^{N_{\text{eff}}} \boldsymbol{v}_{\text{Trans,LHS}_i}\,\boldsymbol{b}_{\alpha_i}^T \tag{2b}$$

$$[C] = m_{\text{sc}}\,[\tilde{\boldsymbol{c}}] + \sum_{i=1}^{N_{\text{eff}}} \boldsymbol{v}_{\text{Rot,LHS}_i}\,\boldsymbol{a}_{\alpha_i}^T \tag{2c}$$

$$[D] = [I_{\text{sc},B}] + \sum_{i=1}^{N_{\text{eff}}} \boldsymbol{v}_{\text{Rot,LHS}_i}\,\boldsymbol{b}_{\alpha_i}^T \tag{2d}$$

$$\boldsymbol{v}_{\text{Trans}} = \boldsymbol{F}_{\text{ext}} - 2m_{\text{sc}}[\tilde{\boldsymbol{\omega}}_{\mathcal{B}/\mathcal{N}}]\boldsymbol{c}' - m_{\text{sc}}[\tilde{\boldsymbol{\omega}}_{\mathcal{B}/\mathcal{N}}][\tilde{\boldsymbol{\omega}}_{\mathcal{B}/\mathcal{N}}]\boldsymbol{c} + \sum_{i=1}^{N_{\text{eff}}}[\boldsymbol{v}_{\text{Trans,RHS}_i} - \boldsymbol{v}_{\text{Trans,LHS}_i}c_{\alpha_i}]$$

$$\tag{3a}$$

$$\boldsymbol{v}_{\text{Rot}} = \boldsymbol{L}_B - [\tilde{\boldsymbol{\omega}}_{\mathcal{B}/\mathcal{N}}]\,[I_{\text{sc},B}]\,\boldsymbol{\omega}_{\mathcal{B}/\mathcal{N}} - [I'_{\text{sc},B}]\boldsymbol{\omega}_{\mathcal{B}/\mathcal{N}} + \sum_{i=1}^{N_{\text{eff}}}[\boldsymbol{v}_{\text{Rot,RHS}_i} - \boldsymbol{v}_{\text{Rot,LHS}_i}c_{\alpha_i}] \tag{3b}$$

Where $m_{\text{sc}}$ is the total mass of the spacecraft, $\boldsymbol{c}$ is the vector from body fixed point $B$ to the center of mass (COM) of the spacecraft $C$, and $[I_{\text{sc},B}]$ is the inertia tensor of the spacecraft about point $B$. Additionally, $N_{\text{eff}}$ is the number of effectors to be summed over, $\boldsymbol{F}_{\text{ext}}$ is the total external force applied to the spacecraft, and $\boldsymbol{L}_B$ is the total external torque applied to the spacecraft. $\boldsymbol{v}_{\text{Trans,RHS}_i}$ and $\boldsymbol{v}_{\text{Rot,RHS}_i}$ are the vector contribution to the forces and torques respectively of effector i, and $\boldsymbol{v}_{\text{Trans,LHS}_i}$ and $\boldsymbol{v}_{\text{Rot,LHS}_i}$ are the vectors for the translational and rotational equations respectively that correspond with effector i's second order derivative of its state. Finally, $\boldsymbol{a}_{\alpha_i}$, $\boldsymbol{b}_{\alpha_i}$, and $c_{\alpha_i}$ are the coefficients from the EOM of effector i relating its second order state $\ddot{\alpha}_i$ to the second order hub translational and rotational states as shown in Eq. (4).

$$\ddot{\alpha}_i = \boldsymbol{a}_{\alpha_i} \cdot \ddot{\boldsymbol{r}}_{B/N} + \boldsymbol{b}_{\alpha_i} \cdot \dot{\boldsymbol{\omega}}_{\mathcal{B}/\mathcal{N}} + c_{\alpha_i} \tag{4}$$

## ADD SELECT BRANCHING TO STATE EFFECTOR

Now knowing the required form of the EOMs of the spacecraft hub and its components for an architecture in which all components are mounted directly to the hub, specific terms can be altered to instead enable linking a component to another component. First focusing on the dynamic effector which contributes external forces and torques to the spacecraft without any states $\alpha_i$ of its own to be integrated. These forces and torques are previously summed up as $\boldsymbol{F}_{\text{ext}}$ and $\boldsymbol{L}_B$ in Eqs. (3a) and (3b) for the hub motion assuming that those forces and torques are transferred to the hub without loss. Instead, the external forces and torques must now be accounted for in the EOM of intermediate platform first.

With Basilisk's spinning bodies chosen as the intermediate platform, its back-substitution formulated EOM from reference 19 for a single rotating segment is shown in Eqs. (5)-(9) with the additional term from all attached components highlighted in blue. Without loss of generality this derivation of a single rotating segment can also be performed for multiple segments.

$$\ddot{\theta} = \boldsymbol{a}_\theta \cdot \ddot{\boldsymbol{r}}_{B/N} + \boldsymbol{b}_\theta \cdot \dot{\boldsymbol{\omega}}_{B/N} + c_\theta \tag{5}$$

$$\boldsymbol{a}_\theta = \frac{m_\mathrm{S}}{m_\theta}[\tilde{\boldsymbol{r}}_{S_c/S}]\hat{\boldsymbol{s}} \tag{6}$$

$$\boldsymbol{b}_\theta = -\frac{1}{m_\theta}\left([I_{\mathrm{S},S}] - m_\mathrm{S}[\tilde{\boldsymbol{r}}_{S/B}][\tilde{\boldsymbol{r}}_{S_c/S}]\right)\hat{\boldsymbol{s}} \tag{7}$$

$$c_\theta = \frac{1}{m_\theta}(u_\mathrm{S} - \hat{\boldsymbol{s}}^T(\boldsymbol{L}_\mathrm{S} + [\tilde{\boldsymbol{\omega}}_{S/N}][I_{\mathrm{S},S}]\boldsymbol{\omega}_{S/N} + [I_{\mathrm{S},S}][\tilde{\boldsymbol{\omega}}_{B/N}]\boldsymbol{\omega}_{S/B}$$
$$+ m_\mathrm{S}[\tilde{\boldsymbol{r}}_{S_c/S}][\tilde{\boldsymbol{\omega}}_{B/N}]\dot{\boldsymbol{r}}_{S/B})) \tag{8}$$

$$m_\theta = \hat{\boldsymbol{s}}^T[I_{\mathrm{S},S}]\hat{\boldsymbol{s}} \tag{9}$$

The platform's state is its angle orientation $\theta$ about axis $\hat{\boldsymbol{s}}$ in the platform's local body fixed frame $\mathcal{S}$ at point S. The mass of the spinning body is $m_\mathrm{S}$ with its COM at point $S_c$ and the mass-like term $m_\theta$ is divided through to isolate the state variable. There is a control torque $u_\mathrm{S}$ for actuated control of the spinning body's orientation, and now an additional torque $L_\mathrm{S}$ representing the total torque from attached components about local frame origin S. The component of the torque parallel to the spin axis is isolated here through its dot product with the spin axis $\hat{\boldsymbol{s}}$. The total external torque on the vehicle must also be accumulated through $\boldsymbol{v}_{\mathrm{Rot,RHS}}$ in the equation updated from reference 19 shown in Eq. (10). Added terms are again highlighted in blue.

$$\boldsymbol{v}_{\mathrm{Rot,RHS}} = -[\tilde{\boldsymbol{\omega}}_{S/N}][I_{\mathrm{S},S_c}]\boldsymbol{\omega}_{S/B} - m_\mathrm{S}[\tilde{\boldsymbol{\omega}}_{B/N}][\tilde{\boldsymbol{r}}_{S_c/B}]\boldsymbol{r}'_{S_c/B}$$
$$- m_\mathrm{S}[\tilde{\boldsymbol{r}}_{S_c/B}][\tilde{\boldsymbol{\omega}}_{S/B}]\boldsymbol{r}'_{S_c/S} + \boldsymbol{L}_\mathrm{S} + [\tilde{\boldsymbol{r}}_{S/B}]\boldsymbol{F}_\mathrm{S} \tag{10}$$

Also present in Eq. (10) is an additional torque computed from the total force contributed by attached components $F_\mathrm{S}$. This force does not appear in the individual EOM for the spinning body state $\theta$ as the torque output from dynamic effectors already accounts for torques imparted by the forces it generates. However, this torque $L_\mathrm{S}$ as suggested by its subscript is computed about local frame origin S, and the torque contributed to $\boldsymbol{v}_{\mathrm{Rot,RHS}}$ is applied about body frame origin B. This total force imparted by attached components $F_\mathrm{S}$ is also factored into the updated equation for $\boldsymbol{v}_{\mathrm{Trans,RHS}}$ as highlighted in blue in Eq. (11).

$$\boldsymbol{v}_{\mathrm{Trans,RHS}} = -m_\mathrm{S}[\tilde{\boldsymbol{\omega}}_{S/B}]\boldsymbol{r}'_{S_c/S} + \boldsymbol{F}_\mathrm{S} \tag{11}$$

This mathematical formulation has been derived in a frame-agnostic way, but in implementation in Basilisk will have frames assigned for each specific vector. It is important that frames are held consistent throughout the equation, and in the existing Basilisk framework

the local body frame $\mathcal{B}$ is chosen when computing back-substitution parameters. Because of this, the forces and torques output by dynamic effectors are produced in its local parent frame which has traditionally been the body frame. However, with this new branching of the dynamic effectors off of state effectors, that local parent frame is not the body frame, and the state effector must rotate these collected forces and torques to the body frame when computing back-substitution parameters.

## NUMERICAL RESULTS

The dynamics of component excited flexing are first demonstrated in Basilisk by a thruster dynamic effector mounted to a 1-DOF spinning body state effector replicating a gimballed thruster. The input parameters corresponding to these components are shown in Table 1, and the spacecraft as well as the spinning body platform start at rest. At ten seconds into the simulation the thruster is turned on at full thrust for thirty seconds and then shut off at forty seconds in.

**Table 1. Simulation parameters for gimballed thruster.**

| Parameter | Notation | Value | Units |
|---|---|---|---|
| Spacecraft mass | $m_{sc}$ | 400 | kg |
| Spacecraft inertia about its COM | $^{\mathcal{B}}[I_{\text{sc},B}]$ | $\begin{bmatrix} 633 & 0 & 0 \\ 0 & 633 & 0 \\ 0 & 0 & 200 \end{bmatrix}$ | kg·m$^2$ |
| Spinning body mass | $m_S$ | 50 | kg |
| Spinning body inertia about its COM | $^{\mathcal{S}}[I_{\text{S},S_c}]$ | $\begin{bmatrix} 50 & 0 & 0 \\ 0 & 30 & 0 \\ 0 & 0 & 40 \end{bmatrix}$ | kg·m$^2$ |
| Spinning body frame origin location in the body frame | $^{\mathcal{B}}\boldsymbol{r}_{S/B}$ | $^{\mathcal{B}}[1,0,0]^T$ | m |
| Spinning body COM in its local frame | $^{\mathcal{S}}\boldsymbol{r}_{S_c/S}$ | $^{\mathcal{B}}[0.5,0,0]^T$ | m |
| Spinning body spin axis in its local frame | $^{\mathcal{S}}\hat{\boldsymbol{s}}$ | $^{\mathcal{S}}[0,1,0]^T$ | m |
| DCM of the $\mathcal{S}$ frame with respect to the $\mathcal{B}$ frame | $[\mathcal{SB}]$ | $\begin{bmatrix} 1 & 0 & 0 \\ 0 & 1 & 0 \\ 0 & 0 & 1 \end{bmatrix}$ | – |
| Spinning body joint stiffness | $k$ | 100 | N·m/rad |
| Spinning body joint damping | $c$ | 50 | N·m·s/rad |
| Thruster position in spinning body frame | $^{\mathcal{S}}\boldsymbol{r}_{T/S}$ | $^{\mathcal{S}}[1,0,0]^T$ | m |
| Thrust direction in spinning body frame | $^{\mathcal{S}}\hat{\boldsymbol{t}}$ | $^{\mathcal{S}}[0,0,-1]^T$ | - |
| Thruster max thrust | $F_{Tmax}$ | 4.5 | N |

Two spacecraft are simulated with these same parameter. One with the new component excited flexing such that the thruster is mounted directly to the flexible platform, and the other using the default methodology in which the thruster is positioned at the same starting location, but applies its forces and torques to the central hub. The resulting motion of the flexible moving platform is shown for both spacecraft in Figure 3.

To study changes in the resulting motion of the spacecraft, Figures 4 through 7 show the

9
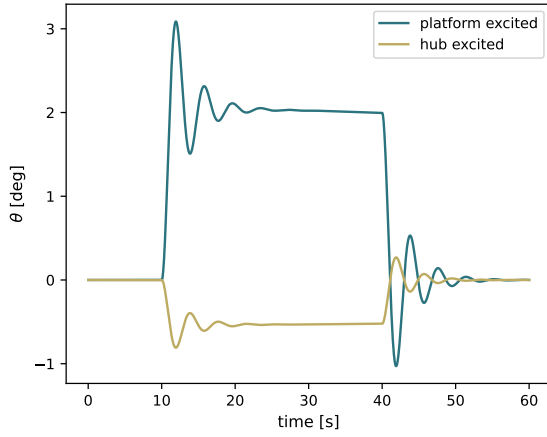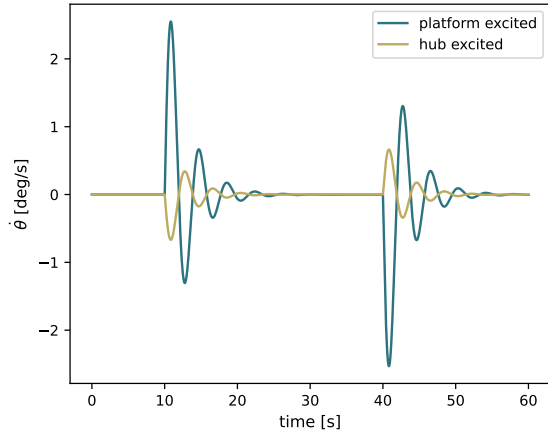
(a) Orientation angle           (b) Orientation angle rate of change

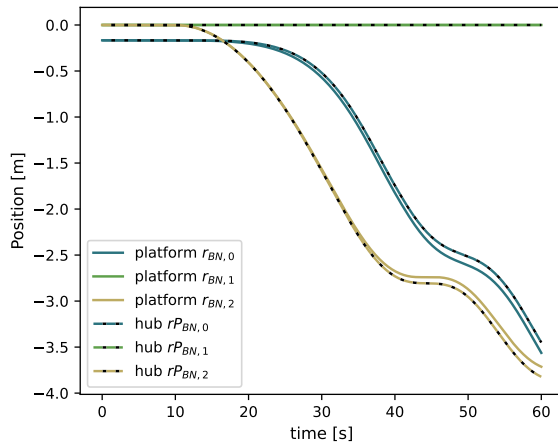**Figure 3.  Spinning body platform motion with thruster firing.**



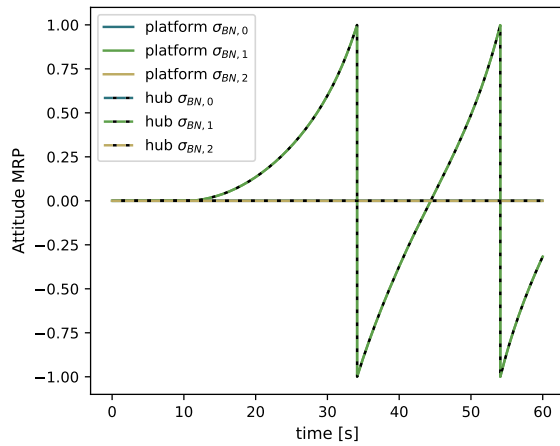**Figure 4.  Hub position with thruster firing.**      **Figure 5.  Hub attitude with thruster firing.**

central hub translational position and velocity as well as attitude and angular rate for the same thruster firing.

## DISCUSSION

The primary benefit of modelling component excited flexing is immediately apparent in Figure 3, in that the resulting deflection of the intermediate platform occurs in the opposing directions. When forces and torques are sent directly to the central hub, the moving platform lags behind in motion, while the actual phenomena is the opposite: that the forces and torques are being applied at the moving platform and it is the central hub which lags behind in motion. Furthermore, the same magnitude of thrust results when applied to the mass of a platform in contrast to the mass of the central hub incites a larger acceleration and therefore a larger deflection of the panel.
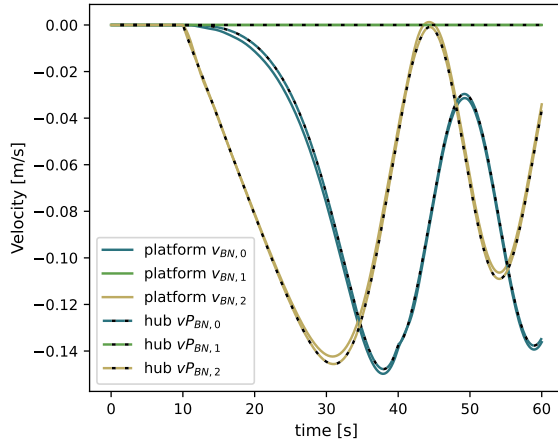
10

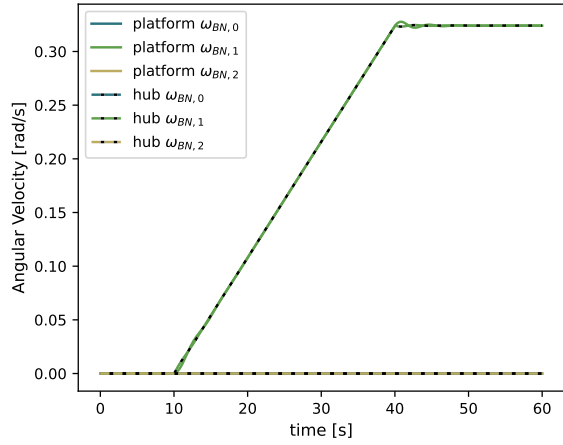**Figure 6. Hub velocity with thruster firing.**



**Figure 7. Hub angular velocity with thruster firing.**

Then studying the resulting motion of the central hub, slight differences in each state are noted. The angular velocity shown in Figure 7 varies during the transients at thruster on and off at ten and forty seconds respectively into the simulation. The associated attitude varies more subtly with angular velocity variations isolated to the transients. The linear velocity shows more appreciable variation past the transient due to the compounded change in force application direction as the attitude drifts, and that drift is compounded further at the translational position differences shown in Figure 4.

## CONCLUSION

This alteration to the BSM surmounts a limitation of Basilisk which previously could not perform branching of components while maintaining its modular architecture. The selective configuration space of branching enables dynamic effectors capable of generating forces and torques to be attached to the spinning bodies state effector capable of modelling rotationally time varying geometries.

While single DOF spinning bodies was adapted to accommodate attached dynamic effectors in this work, an N-DOF spinning bodies state effector now exists which enables a generalized set of spinning bodies of any number of successive platforms. Future work at the back-substitution level aims to adapt the attachment of dynamic effectors to this N-DOF model, enabling an even larger configuration space of branching.

This branching also enables further complexity at the scenario level. Future work of interest includes modelling a moving platform as a more significant portion of the spacecraft such as a dual-spinner which may have multiple components attached to the intermediate platform. Additionally, scenarios can be expanded at the controls level to study the differences in resulting motion and resonance analysis with pulsed thrust control.

# REFERENCES

[1] A. K. Banerjee, "Contributions of Multibody Dynamics to Space Flight: A Brief Review," *Journal of Guidance, Control, and Dynamics*, Vol. 26, No. 3, 2003, pp. 385–394, 10.2514/2.5069.

[2] A. Jain, "Unified formulation of dynamics for serial rigid multibody systems," *Journal of Guidance, Control, and Dynamics*, Vol. 14, No. 3, 1991, pp. 531–542, 10.2514/3.20672.

[3] T. R. Kane and D. A. Levinson, "Formulation of equations of motion for complex spacecraft," *Journal of Guidance and control*, Vol. 3, No. 2, 1980, pp. 99–112.

[4] A. Jain and G. Rodriguez, "Recursive dynamics algorithm for multibody systems with prescribed motion," *Journal of guidance, control, and dynamics*, Vol. 16, No. 5, 1993, pp. 830–837.

[5] L. Kiner, J. V. Carneiro, C. Allard, and H. Schaub, "Spacecraft Simulation Software Implementation of General Prescribed Motion Dynamics of Two Connected Rigid Bodies," *AAS Rocky Mountain GN&C Conference, Breckenridge, CO*, 2023.

[6] C. Allard, H. Schaub, and S. Piggott, "General Hinged Solar Panel Dynamics Approximating First-Order Spacecraft Flexing," *AIAA Journal of Spacecraft and Rockets*, Vol. 55, No. 5, 2018, pp. 1290–1298, 10.2514/1.A34125.

[7] A. Grewal and V. J. Modi, "Multibody dynamics and robust control of flexible spacecraft," *IEEE Transactions on Aerospace and Electronic Systems*, Vol. 36, No. 2, 2000, pp. 491–500.

[8] SpaceLogistics, "Mission Extension Vehicle (MEV) Fact Sheet," 2021.

[9] T. Harris, H. Brettle, M. Lecas, L. Blacketer, A. Carr, A. Fernandez, and A. Puppa, "An exploration of opportunities to advance ground-based and space-based SSA systems through in-orbit demonstration missions," *8th European Conference on Space Debris*, April 2021.

[10] R. Biesbroek, S. Aziz, A. Wolahan, S.-f. Cipolla, M. Richard-Noca, and L. Piguet, "The clearspace-1 mission: Esa and clearspace team up to remove debris," *Proc. 8th Eur. Conf. Sp. Debris*, 2021, pp. 1–3.

[11] S. Space, "Otter is there, on call and ready to support." `https://www.starfishspace.com/the-otter/`, 2023.

[12] M. A. Shoemaker, M. Vavrina, D. E. Gaylor, R. Mcintosh, M. Volle, and J. Jacobsohn, "OSAM-1 decommissioning orbit design," *AAS/AIAA Astrodynamics Specialis t Conference*, 2020.

[13] R. Staples, "Key Capabilities of our Life Extension In-orbit (LEXI™) Servicer," `https://astroscale-us.com/lexi-life-extension-capabilities/`, October 2021.

[14] A. Eisele, "Northrop Grumman's SpaceLogistics Continues Revolutionary Satellite Life-Extension Work with Sale of Third Mission Extension Pod," `https://news.northropgrumman.com/news/releases/northrop-grummans-spacelogistics-continues-revolutionary-satellite-life-extension-work-with-sale-of-third-mission-extension-pod`, June 2023.

[15] B. Wie, N. Furumoto, A. Banerjee, and P. Barba, "Modeling and simulation of spacecraft solar array deployment," *Journal of Guidance, Control, and Dynamics*, Vol. 9, No. 5, 1986, pp. 593–598.

[16] G. Bascom and H. Schaub, "Modular Dynamic Modeling Of Hinged Solar Panel Deployments," *AAS Astrodynamics Specialist Conference*, Charlotte, NC, Aug. 7–10 2022. Paper No. AAS 22-725.

[17] P. W. Kenneally, S. Piggott, and H. Schaub, "Basilisk: A Flexible, Scalable and Modular Astrodynamics Simulation Framework," *Journal of Aerospace Information Systems*, Vol. 17, Sept. 2020, pp. 496–507.

[18] C. Allard, M. Diaz-Ramos, P. W. Kenneally, H. Schaub, and S. Piggott, "Modular Software Architecture for Fully-Coupled Spacecraft Simulations," *Journal of Aerospace Information Systems*, Vol. 15, No. 12, 2018, pp. 670–683, 10.2514/1.I010653.

[19] J. Vaz Carneiro, C. Allard, and H. Schaub, "Rotating Rigid Body Dynamics Architecture For Spacecraft Simulation Software Implementation," *AAS Guidance and Control Conference*, Breckenridge, CO, Feb. 2–8 2023. Paper No. AAS-23-112.